J Comp Physiol A (2008) 194:811–820
DOI 10.1007/s00359-008-0352-0

ORIGINAL PAPER

Cadherin 23-like polypeptide in hair bundle mechanoreceptors of sea anemones

Glen M. Watson · Lankhanh Pham · Erin M. Graugnard · Patricia Mire

Received: 16 January 2008 / Revised: 19 June 2008 / Accepted: 3 July 2008 / Published online: 25 July 2008

Abstract We investigated hair bundle mechanoreceptors in sea anemones for a homolog of cadherin 23. A candidate sequence was identified from the database for *Nematostella vectensis* that has a shared lineage with vertebrate cadherin 23s. This cadherin 23-like protein comprises 6,074 residues. It is an integral protein that features three transmembrane alpha-helices and a large extracellular loop with 44 contiguous, cadherin (CAD) domains. In the second half of the polypeptide, the CAD domains occur in a quadruple repeat pattern. Members of the same repeat group (i.e., CAD 18, 22, 26, and so on) share nearly identical amino acid sequences. An affinity-purified antibody was generated to a peptide from the C-terminus of the cadherin 23-like polypeptide. The peptide is expected to lie on the exoplasmic side of the plasma membrane. In LM, the immunolabel produced punctate fluorescence in hair bundles. In TEM, immunogold particles were observed medially and distally on stereocilia of hair bundles. Dilute solutions of the antibody disrupted vibration sensitivity in anemones. We conclude that the cadherin 23-like polypeptide likely contributes to the mechanotransduction apparatus of hair bundle mechanoreceptors of anemones.

Keywords Hair cell · Tip link · Sensory transduction

Introduction

Hair bundle mechanoreceptors detect sound, vibrations, acceleration and gravity (Hudspeth 1997). According to the gating spring model for signal transduction, a gating spring is attached to the transduction channel. Deflecting the hair bundle in a positive direction (i.e., toward taller stereocilia) imposes strain on the gating spring. Strain on the gating spring opens the channel to permit a cation influx that depolarizes the membrane potential of the hair cell (Hudspeth 1985; Howard et al. 1988; Roberts et al. 1988; Ashmore 1991; see the review by LeMasurier and Gillespie 2005).

Tip links are extracellular linkages interconnecting the tip of one stereocilium with the distal region of the adjacent, taller stereocilium (Pickles et al. 1984; Furness and Hackney 1985; Slepecky and Chamberlain 1985; Osborne et al. 1988). Tip links are helical filaments measuring 150–200 nm long and 8–11 nm thick (Kachar et al. 2000; Tsuprun et al. 2004). Although tip links initially were proposed to be the gating spring, their helical structure suggests that tip links are stiff and hence unlikely to be the gating spring (Kachar et al. 2000; Tsuprun et al. 2004; Sotomayor et al. 2005). Nevertheless, tip links are essential to signal transduction. Tip links are disrupted upon immersing hair cells in calcium-depleted buffers or upon digestion by elastase (Assad et al. 1991; Preyer et al. 1995). A loss of tip links is accompanied by a loss of mechanosensitivity. In chickens, missing tip links and mechanosensitivity are restored within approximately 12 h after returning the hair cells to calcium-containing buffer (Zhao et al. 1996). Thus, the presence of tip links and mechanosensitivity are positively correlated.

In zebrafish, mutants for the gene encoding cadherin 23 lack tip links and functional hair cells (Sollner et al. 2004; Nicolson et al. 1998). In mammals, defects in the gene encoding cadherin 23 result in a deafness syndrome, Usher 1D (Bork et al. 2001; Bolz et al. 2001; Di Palma et al. 2001). Antibodies to cadherin 23 labeled linkages interconnecting stereocilia in developing hair cells but not in mature

G. M. Watson (✉) · L. Pham · E. M. Graugnard · P. Mire
Department of Biology, University of Louisiana at Lafayette, Lafayette, LA 70504-2451, USA
e-mail: gmw5722@louisiana.edu

hair bundles (Michel et al. 2005; Lagziel et al. 2005). A different antibody to cadherin 23 labeled the tips of stereocilia in mature hair bundles, suggesting that cadherin 23 is a major component of tip links (Siemens et al. 2004). In zebrafish, cadherin 23 is a single pass, integral protein with 27 cadherin domains (CAD, Sollner et al. 2004; Siemens et al. 2004). Each CAD consists of approximately 110 residues. Calcium binding motifs located at each end of the CAD stabilize its conformation (Sotomayor et al. 2005). The expected dimensions of cadherin 23 are consistent with tip links measured from electron micrographs provided that cadherin 23 self-associates into transmultimers to form tip links (Tsuprun et al. 2004). Presumably, a *cis*-homodimer from each stereocilium forms a *trans*-association to complete the tip link. However, it also has been proposed that tip links include protocadherin 15 (Ahmed et al. 2006). Protocadherin 15 consists of a single pass, integral protein having 11 CAD domains (Ahmed et al. 2006). Apparently, in mammals tip links consist of a *trans*-heterotetramer of cadherin 23 at the distal end and protocadherin 15 at the proximal end (Kazmierczak et al. 2007).

Sea anemones are marine invertebrates that employ hair bundle mechanoreceptors on their tentacles to detect swimming prey (Watson and Hessinger 1989; Watson and Mire 2004). Anemone hair bundles are derived from a multicellular complex featuring a sensory neuron at its center. From the sensory neuron extends a single kinocilium surrounded by 6–7 large diameter stereocilia. Two to four non-neuronal cells functioning as hair cells surround the sensory neuron. Approximately 200–300 small diameter stereocilia arising from the hair cells converge onto the large diameter stereocilia (Peteya 1975; Mire-Thibodeaux and Watson 1994). The stereocilia are interconnected by tip links among other linkages. Tip links in anemones are similar in morphology to tip links in vertebrates (Watson et al. 1997). Mechanosensitivity is disrupted after exposing sea anemones either to calcium-depleted seawater or to elastase (Watson et al. 1998a). The purpose of the present study is to investigate the possibility that anemone hair bundles include a homolog of cadherin 23.

Materials and methods

Animal maintenance

Sea anemones, *Haliplanella luciae,* were maintained in shallow glass dishes containing natural seawater at 32°/$_{oo}$ and 16°C. Anemones, *Nematostella vectensis*, were maintained in shallow glass dishes in diluted seawater at 16°/$_{oo}$ and 22°C, but were otherwise maintained as for *Haliplanella*. The animals were fed to repletion twice weekly using freshly hatched *Artemia* nauplii (Minasian and Mariscal 1979). Feeding was followed by a change in seawater.

Immunocytochemistry

Specimens of *H. luciae* were anesthetized in KSW (in mM concentrations: NaCl 323; $MgSO_4$ 26; $MgCl_2$ 24; KCl 100; $CaCl_2$ 12; and $NaHCO_3$ 2) for 1.5 h. Specimens of *N. vectensis* were anesthetized in half strength KSW. The animals were fixed using 0.05% glutaraldehyde and 4% paraformaldehyde prepared in Millonig buffer augmented with 3% NaCl for 30 min (or 1.5% NaCl for *Nematostella*) at room temperature. Specimens were rinsed in PBS and then blocked in 3% bovine serum albumin, BSA in phosphate buffered saline, PBS (BSA/PBS). Specimens were incubated in a 1/100 to 1/25 dilution of an affinity-purified anti-cadherin 23 antibody developed in chickens (Alpha Diagnostics International, San Antonio, TX, USA) in BSA/PBS overnight at 4°C. A synthetic peptide antigen was used corresponding to residues 6058-6074 and consisting of the following sequence: (C)SEMDMTYDAYRYDETTL. Following the incubation in the primary antibody, the tissue was rinsed in PBS, blocked in BSA/PBS and then incubated in anti-chicken IgG conjugated to AlexaFluor 488 or AlexaFluor 555 (Invitrogen, Molecular Probes, Eugene, OR, USA) in BSA/PBS for 30–60 min. The tissue was rinsed in PBS and then transferred to 100 μM citric acid in PBS to retard bleaching. Excised tentacles were prepared as wet mounts and then imaged using an LOMO Lumam epifluorescent microscope (model RP011-T, LOMO America, Prospect Heights, IL, USA). The principal objective used was a 100× oil-immersion fluorite (na = 1.30). Images were obtained using an STL-11000 SBIG cooled CCD camera (SBIG, Santa Barbara, CA, USA) controlled by Maxim-DL software (Diffraction Limited, ON, Canada). Immunoelectron microscopy was performed as follows. Anesthetized specimens of *Haliplanella* were fixed in 0.025 to 0.05% glutaraldehyde and 4% paraformaldehyde in Millonig buffer containing 3% NaCl for 30 min. Remaining free aldehydes of glutaraldehyde were blocked by immersing the tissue in 0.1 M glycine in PBS for 5 min. In some cases, antigen retrieval was performed by incubating the tissue in 0.005% citraconic anhydride in PBS at 90°C for 60 min (Namimatsu et al. 2005). The tissue was rinsed in PBS for 5 min and then incubated in BSA/PBS for 30 min to block nonspecific binding sites. The tissue was incubated overnight in a 1/100 to 1/25 dilution of affinity-purified anti-cadherin 23-like polypeptide in BSA/PBS at 4°C. The tissue was rinsed in PBS, blocked in BSA/PBS, and then incubated in anti-chicken IgG conjugated to colloidal gold diluted 1/25 in BSA/PBS overnight at 4°C. The tissue was rinsed in PBS for 30 min and then fixed in 1% glutaraldehyde in PBS for 1 h. The tissue was rinsed in PBS, then dehydrated in acetone and embedded in Spurr resin. Thin sections were osmicated for 10 min on drops of 0.04% OsO_4 and then counterstained in 1% uranyl acetate for 1 h

and a triple lead stain for 5 min. Sections were viewed using a Hitachi 7000 TEM operating at 75 kV. Field emission scanning electron microscopy was performed using methods described earlier (Mire and Nasse 2002). Digital images were noise filtered and contrast adjusted. In addition, in some images details were sharpened by employing a Lucy–Richardson deconvolution algorithm.

Sequence analysis

The amino acid sequences of proteins downloaded from NCBI (http://ncbi.nlm.nih.gov) were compared from the anemone sequence from the *Nematostella* database (http://www.stellabase.org) using the Megalign module of Lasergene software using the ClustalW algorithm set to the slow/accurate setting (DNASTAR, Madison, WI, USA).

Nematocyst discharge bioassay

In this bioassay, gelatin-coated strands of fishing line (test probes) are briefly hydrated and then touched to tentacles of anemones. The test probes are fixed in glutaraldehyde and then imaged using phase contrast optics. Microbasic p-mastigophore nematocysts discharged into the gelatin coating are counted for a single field of view at 400× total magnification (Watson et al. 1998b). Anemones (*H. luciae*) were incubated in seawater containing a 1/3,000 dilution of the affinity-purified antibody to the cadherin 23-like polypeptide (or not for untreated controls). The antibody was premixed in seawater and then used to replace seawater in the dish containing the specimens. For the first 20 min of exposure to the antibody solution, anemones were touched with test probes in the presence of vibrations at 55 Hz, one of the several key frequencies that elicit maximal discharge of nematocysts (Watson et al. 1998b). Discharge was tested at 5 min increments beginning at 5 min exposure to the antibody solution. At 25 min exposure to the antibody solution, discharge was tested in the absence of vibrations to determine whether baseline discharge was affected by the antibody. The untreated controls were handled in a manner identical to that for the antibody-treated anemones except for the presence of the antibody. Thus, for untreated control animals, the seawater bathing the anemones was replaced with fresh seawater before nematocyst discharge was tested at specified increments. At each time point, a total of 10 test probes were obtained from two replicate experiments performed on different days. The data were pooled and then analyzed statistically by ANOVA followed by LSD post hoc tests using CSS Statistica software (Statsoft, Tulsa, OK, USA). Like comparisons were made (i.e., data for 5 min min exposure to the antibody were compared to data for 5 min controls). Significant differences appear as asterisks on graphs plotted using Origin software (Microcal Software, Northampton, MA, USA).

Results

The peptide sequence of cadherin 23 from zebrafish, *Danio rerio,* (accession number NP999974) was used to screen the StellaBLAST database for the model sea anemone, *N. vectensis,* for related peptide sequences. The candidate that shared the closest identity with the zebrafish cadherin 23 was SB 58036 (http://www.stellabase.org). This polypeptide is predicted to comprise 6,074 residues including a single Ig domain followed by 44 CAD domains (Fig. 1) (http://pfam.sanger.ac.uk/). The polypeptide is an integral protein with three membrane-spanning alpha-helices (http://www.enzim.hu/hmmtop). The N-terminus is cytoplasmic with 361 residues located in the cytoplasm. The cytoplasmic domain does not share significant homology with cytoplasmic domains of other cadherins. From the N-terminus, a membrane-spanning alpha helix leads to a large extracellular domain that forms a loop consisting of the Ig domain and the CAD domains. The polypeptide re-enters the cytoplasm by means of the second membrane-spanning alpha helix with a short cytoplasmic loop leading to the last membrane-spanning helix. The extracellular C-terminus consists

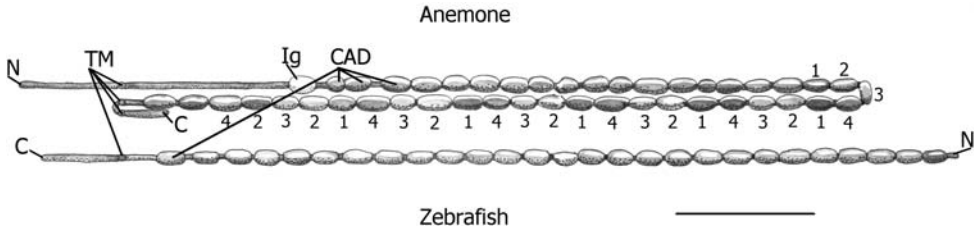

Fig. 1 Domain structure of cadherin 23 in sea anemones and zebrafish. The domain structure is plotted for SB 58036, a cadherin 23-like polypeptide in anemones and cadherin 23 in zebrafish based on the primary structure of the polypeptides. The ends of the polypeptides residing in the cytoplasm are pictured at *left*. Transmembrane domains (*TM*) are indicated with the majority of the polypeptides extending into the extracellular space. In the anemone polypeptide, an Ig domain (*Ig*) precedes 44 contiguous cadherin domains (*CAD*). A quadruple repeat pattern is evident in some of the CAD domains and numbered accordingly. In the zebrafish cadherin 23, contiguous CAD domains occur in the extracellular space. Amino-terminal ends (*N*) and carboxy-terminal ends (*C*) of the polypeptides are indicated. *Scale bar* 500 residues

of 167 residues. The polypeptide is shown diagrammatically in Fig. 1. A reverse BLAST showed that SB 58036 shares homology with FAT4 cadherin in addition to cadherin 23. A phylogenetic tree was constructed using sequence information for cadherin 23, FAT4 and protocadherin 15 from a variety of vertebrate and invertebrate animals (Fig. 2). The tree indicates that SB 58036 shares a common, albeit distant ancestor with the cadherin 23s and cadherin 23-like proteins. Evidently, the anemone sequence is more closely related to the cadherin 23s than to the FAT4 cadherins or to the protocadherin 15s from model vertebrates (Fig. 2). A representative sequence alignment of CAD domains from *Nematostella* and *Danio* is shown in Fig. 3. Areas that are identical to the consensus sequence are commonplace among the four sequences. Thus, the anemone CADs appear to be typical of CADs in vertebrate proteins. Interestingly, in *Nematostella*, the CAD domains in the second half of the polypeptide occur in a quadruple repeat pattern beginning with the 18th CAD domain. The amino acid sequence of the *Nematostella* CAD domains is highly consistent among members of the same repeat group (at every fourth CAD domain). This is shown diagrammatically in Fig. 1 and also by a phylogenetic tree based on an alignment of the excised CADs from SB 58036 (Fig. 4). No quadruple repeat pattern is present among the 27 CADs in the zebrafish cadherin 23.

A reference FESEM micrograph of a hair bundle located on a tentacle of *H. luciae* is shown in Fig. 5. Numerous small diameter stereocilia converge onto longer, large diameter stereocilia located at the center of the hair bundle. In anemones, hair bundles are radially symmetric. Polyclonal antibodies were raised to the extracellular C-terminus of *Nematostella's* cadherin 23-like polypeptide. The antibodies label hair bundles in *Nematostella* with punctate fluorescence (Fig. 6a). The oblique contrast transmitted light microscope image is shown for the same hair bundle in Fig. 6b and the merged image in Fig. 6c. A similar labeling pattern occurs for hair bundles of the anemone *H. luciae* (Fig. 6d–f), the species of anemone for which the sensory physiology of hair bundles is well studied. A top view of the hair bundles reveals that the immunolabel extends across the entire hair bundle (Fig. 6g–i). Secondary only controls are negative insofar as they lack the punctate fluorescence (Fig. 6j–l). The punctate fluorescence shown in Fig. 6 does not indicate where the immunodetection of the cadherin 23-like polypeptide occurs along the length of individual stereocilia because small diameter stereocilia can partner with taller neighboring stereocilia along the

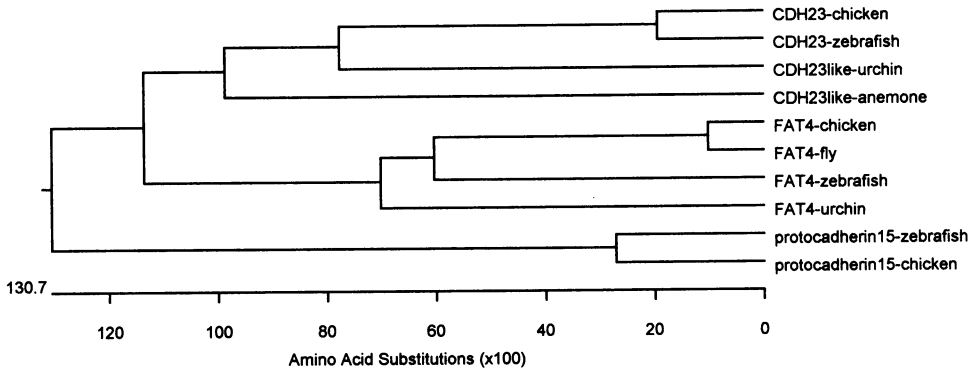

Fig. 2 Phylogenetic tree comparing SB 58036 to cadherin 23, FAT 4 cadherin and protocadherin 15 from selected vertebrate and invertebrate animals. The downloaded amino acid sequences were aligned using Lasergene Megalign software based on a Clustal W algorithm. SB 58036 is a cadherin 23-like polypeptide from the model anemone *Nematostella*; cadherin 23 from zebrafish (Accession number NP999974); and chickens (XP421595); a cadherin 23-like polypeptide from sea urchins (XP001189008); FAT4 cadherin from flies (EAX05203); chickens (XP420617); zebrafish (XP001178338); sea urchins (XP001178338); and protocadherin 15 from zebrafish (NP001012500); and chickens (NP001038119)

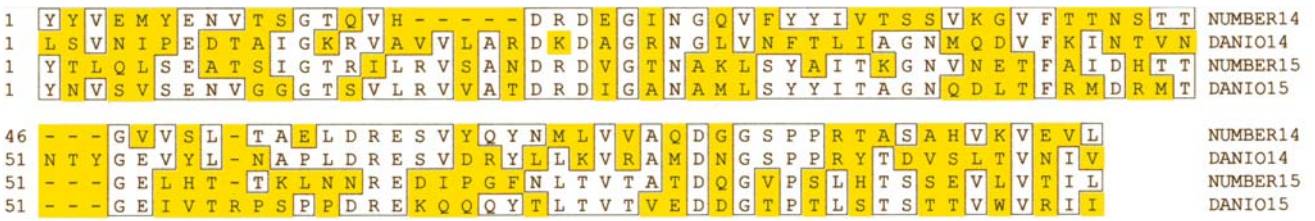

Fig. 3 Sequence alignment of cadherin repeat domains (CADs) from *Nematostella* and *Danio*. Excised CADs from *Nematostella* (*Numbers 14, 15*) were aligned with excised CADs from zebrafish (*Danio 14, 15*). Residues that are identical with the consensus sequence are *boxed in*.

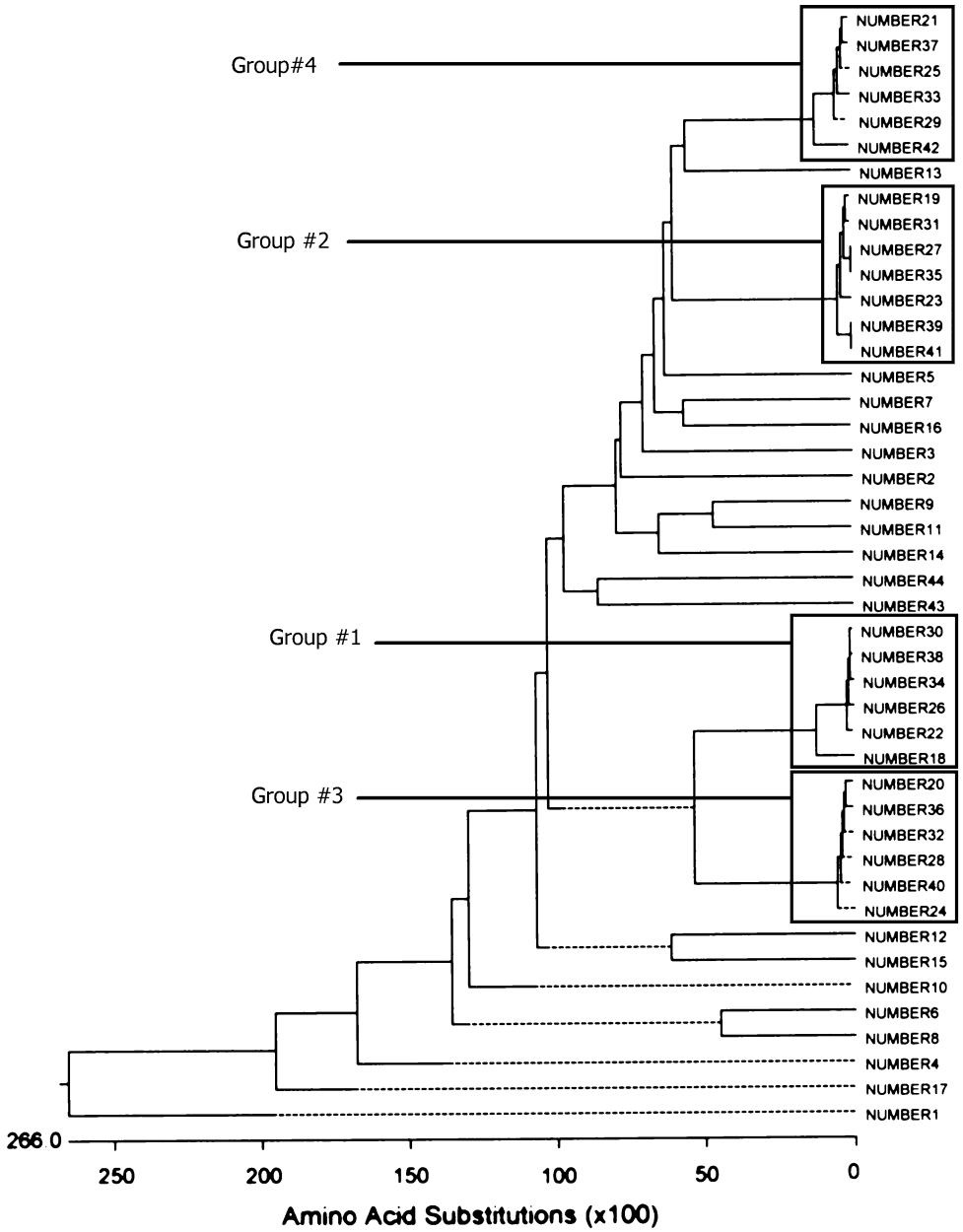

Fig. 4 Phylogenetic tree comparing excised CADs from SB 58036. The CADs were identified after entering the amino acid sequence of SB58036 into the pfam server. Excised CADs were aligned using the megalign module of Lasergene software. The tree was produced using the ClustalW algorithm set to the slow-accurate setting. Cadherin repeat groups are *numbered 1–4* on the phylogenetic tree

length of the hair bundle (e.g., Fig. 5). To resolve this issue, immunoelectron microscopy was performed. For specimens fixed in 0.05% glutaraldehyde and 4% paraformaldehyde, antigen retrieval was necessary. Immunogold particles occurred singly and in small clusters on stereocilia, a representative example of which is shown in Fig. 7. Gold particles were counted and scored according to their location. Most of the gold particles occurred on small diameter stereocilia, which in anemone hair bundles are more abundant than large diameter stereocilia. However, gold particles occurred on both types of stereocilum. Of a total of 588 particles counted, 47.6% occurred distally on stereocilia, 43.7% medially and 4.5% occurred basally on stereocilia (Fig. 8). The medial compartment was approximately two to three times larger than either the distal or basal compartments. The distal and basal compartments were similar in size to each other. Hence, the 43.7% medial label was distributed over a larger area than for the distal or basal label. Approximately 4.1% of the gold particles were observed on cell surfaces other than stereocilia (Fig. 8). Gold particles were observed in pairs of stereocilia within 150–200 nm of the tip of the shorter stereocilium. Such a distribution is consistent for the immunolabel to be in the vicinity of insertion points for tip links (Watson et al. 1997). In most cases, the gold particles occurred in small clusters on the taller stereocilum (Fig. 9a, b). In one case, a single gold particle occurred at each end of a linkage, possibly a tip link (Fig. 9c).

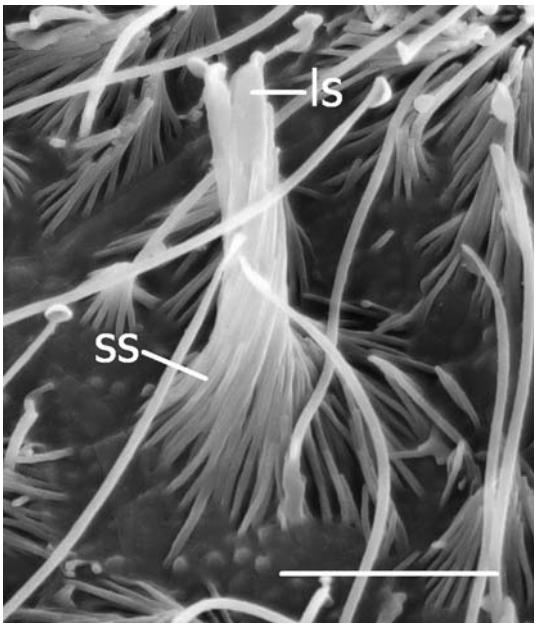

Fig. 5 Hair bundle from *Haliplanella luciae*. A hair bundle arising from the surface of a tentacle is shown in FESEM. Small diameter stereocilia (*ss*) converge onto large diameter stereocilia (*ls*). *Scale bar* 5 μm

We were interested in determining whether a lower glutaraldehyde concentration would produce satisfactory results without the necessity of antigen retrieval. A single specimen was fixed in 0.025% glutaraldehyde and 4% paraformaldehyde without antigen retrieval and processed as follows: one-third was processed for routine immunogold microscopy, i.e., exposed to the primary antibody followed by the secondary antibody conjugated to colloidal gold (experimental, Fig. 10); one-third was exposed to the primary antibody in the presence of the peptide antigen at a final concentration of 1 mg/ml followed by the secondary antibody conjugated to colloidal gold (peptide control, Fig. 10) and one-third was exposed only to the secondary antibody conjugated to colloidal gold (secondary control, Fig. 10). The experimental tissue was immuno-labeled in a fashion consistent with that shown in Figs. 7 and 9. To determine the specificity of the label, immunogold particles were counted for comparable areas of thin sections viewed by TEM. Of a total of 519 gold particles counted, 88.4% occurred in the experimental tissue. Only three gold particles occurred in the secondary controls (Fig. 10). Thus, the primary antibody exhibits reasonable specificity.

Because the antigen-binding site at the C-terminus of SB 58036 is expected to be exposed to seawater, we tested the effects on vibration sensitivity of adding the affinity-purified antibody to the seawater containing the anemones. At an antibody dilution of 1/3,000, discharge of nematocysts in the presence of vibrations at 55 Hz significantly decreases by 10 min exposure to the antibody (Fig. 11). By 15 min exposure to the antibody, levels of discharge are virtually identical to those for nonvibrating controls. Note that even after 25 min exposure the antibody solution, discharge of nematocysts at 0 Hz (in the absence of vibrations) is comparable to that for untreated controls (Fig. 11).

Discussion

The genome of the model sea anemone, *Nematostella*, contains a total of 46 genes encoding cadherins as compared to 127 cadherin genes in the genome of mice (Abedin and King 2008). Currently, we are interested in 5 'large' cadherins comprising 4,578 ± 530 residues (mean ± SEM), including SB 58036, as candidates for involvement in signal transduction of hair bundles. A phylogenetic tree comparing SB 58036 to cadherin 23, FAT4 cadherin and protocadherin 15 suggests that SB 58036 is a cadherin 23-like polypeptide. SB 58036 is localized to hair bundle mechanoreceptors. At the light microscopic level, the immunolabel produces punctate fluorescence. At the electron microscopic level, approximately one-half of the immunolabel is located distally on stereocilia. This immunolabel is in the proper location to contribute to the structure of tip links. Another 40% of the total label is located medially in stereocilia. At least some of the medial immunolabel may also contribute to the structure of tip links because, in anemone hair bundles, stereocilium pairs can be dissimilar in length with short stereocilia converging onto longer stereocilia nearly twice their length (see Fig. 5). In immunoelectron microscopy, some images of intact pairs of stereocilia had gold particles in areas where the insertion points of tip links would be expected to occur. We conclude that the anemone cadherin 23-like polypeptide is located in the appropriate area of the hair bundle to contribute to the structure of tip links.

The cadherin 23-like polypeptide in anemones is unusual in structure as compared to cadherin 23 in model vertebrates such as zebrafish. First, the anemone protein is nearly twice as large as in zebrafish with nearly twice as many CAD domains. Conceivably, this observation might be generalized to other cadherins since, in *Nematostella,* cadherins have an average of 11 CADs as compared to 5.2 CADs in mice (Abedin and King 2008). Second, the cadherin 23-like polypeptide has three transmembrane domains rather than one in cadherin 23 of zebrafish. The first transmembrane domain is located near to the N-terminus and the other two transmembrane domains are clustered together near the C-terminus. The intervening sequence contains the 44 CAD domains folded into a large extracellular loop.

In sea anemones, hair bundles participate in the regulation of discharge of nematocysts during prey capture. Nematocysts are specialized secretory products that consist

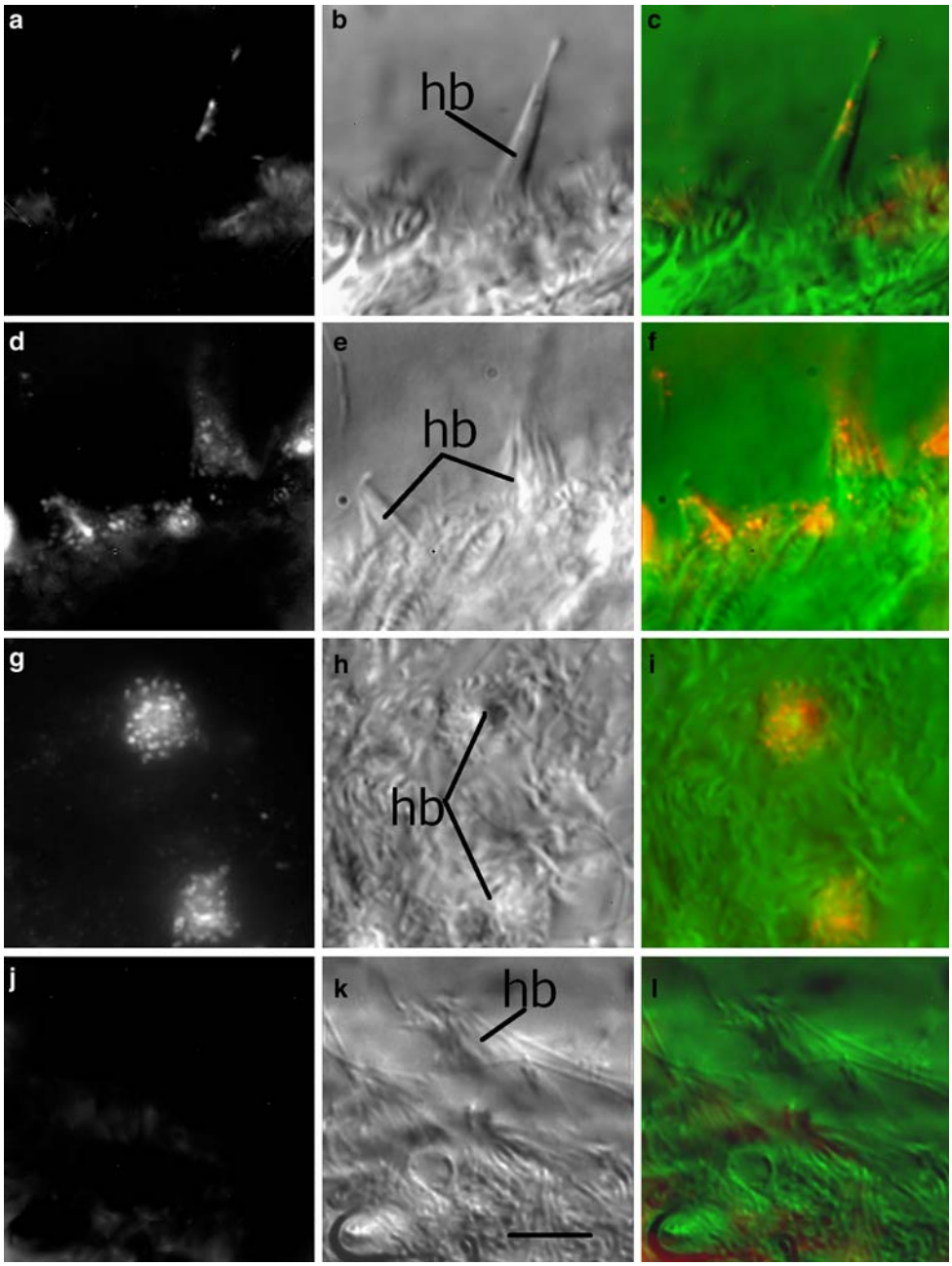

Fig. 6 Cadherin 23-like immunocytochemistry of hair bundles. A peptide derived from the sequence of SB 58036 was used to immunize chickens. An affinity-purified polyclonal antibody was used in immunocytochemistry. In **a** immunofluorescence is shown for a hair bundle arising from the tentacle surface of the sea anemone, *Nematostella vectensis*. The hair bundle is viewed in profile. In **b** the same hair bundle (*hb*) from **a** is shown by oblique contrast microscopy. In **c** a composite image shows a merged image from **a** and **b**. In **d** immunofluorescence is shown for hair bundles arising from the tentacle surface of the sea anemone, *Haliplanella luciae*. The hair bundles are viewed in profile. In **e** the same hair bundles (*hb*) from panel **d** are shown by oblique contrast microscopy. In **f** a composite image shows a merged image from panels **d** and **e**. In **g** immunofluorescence is shown in *top view* looking down upon two hair bundles arising from the tentacle surface of the sea anemone, *Haliplanella luciae*. In **h** the same hair bundles (*hb*) from **g** are shown by oblique contrast microscopy. In **i** a composite image shows a merged image from **g** and **h**. In **j** a secondary only control is shown for the sea anemone, *Haliplanella luciae*. In **k** the same hair bundle (*hb*) from **j** is shown by oblique contrast microscopy. In **l** a composite image shows a merged image from panels **j** and **k**. *Scale bar* 5 μm

of a capsule containing an inverted tubule. Nematocysts forcibly evert the tubule in a process known as 'discharge' (Mariscal 1974). In the absence of vibrations, or in the presence of vibrations at non-key frequencies, a baseline number of nematocysts is discharged into test probes touched to tentacles. In the presence of vibrations at key frequencies, including 55 Hz, levels of discharge increase to 1.5 to 2 times baseline (Watson et al. 1998b). Thus, vibration-dependent discharge increases above baseline discharge that always is present. Dilute affinity-purified antibody added to the seawater containing the anemones causes a gradual loss of vibration sensitivity. Note that in the presence of the antibody, levels of discharge decrease to baseline (obtained at 0 Hz), but not below. A similar loss of vibration-dependent discharge, but not baseline discharge of nematocysts, is observed following treatment of anemones in aminoglycoside antibiotics (Watson et al. 1997) or in agents that disrupt tip links including elastase or calcium-depleted seawater (Watson et al. 1998a). The effects of the antibody on discharge suggest that the cadherin 23-like polypeptide in anemones is likely to be involved in the signal transduction pathway linking vibration detection to nematocyst discharge. Because the antibody to the cadherin 23-like polypeptide localizes to hair bundles in the vicinity of tip links, it appears that such involvement occurs early in the pathway, perhaps at the point of signal transduction.

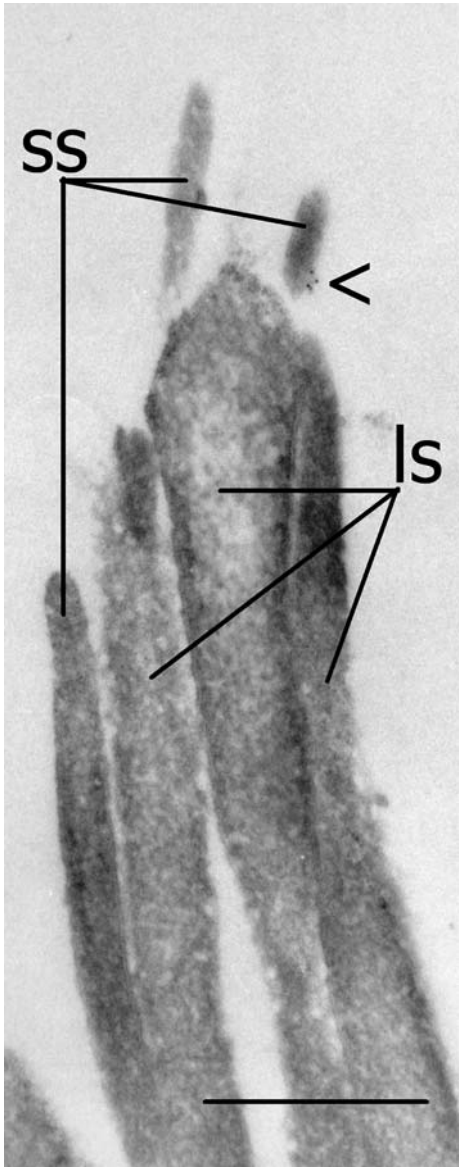

Fig. 7 Cadherin 23-like immunoelectron microscopy of an anemone hair bundle. Tissue from the anemone, *Haliplanella luciae*, was processed for pre-embedment immunoelectron microscopy. Immunogold particles appear distally (*arrowhead*) on small diameter stereocilia (*ss*). Small diameter stereocilia converge onto large diameter stereocilia (*ls*) of the same hair bundle. *Scale bar* 0.39 μm

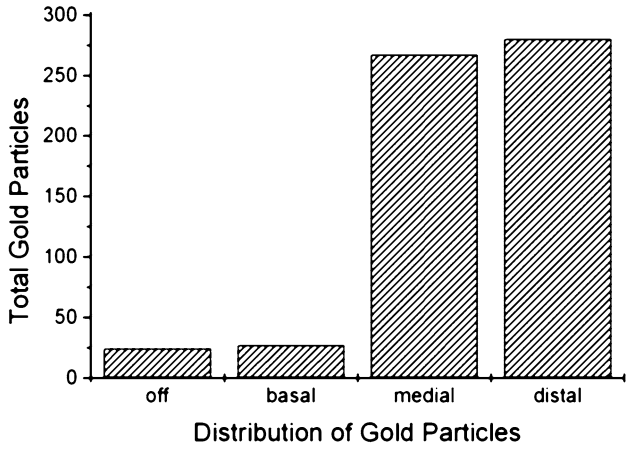

Fig. 8 Spatial distribution of cadherin 23-like immunogold particles. Immunogold particles were counted and plotted according to their distribution along the length of stereocilia; distal; medial; and basal of hair bundles from the sea anemone, *Haliplanella luciae*. In addition, immunogold particles that were counted on the surfaces of other cells were plotted in the category; *off* indicating their location is 'off' of stereocilia

Thus, the cadherin 23-like polypeptide might be a component of the mechanotransduction apparatus of hair bundles in sea anemones.

Aminoglycosides and agents that disrupt tip links have relatively rapid effects on mechanotransduction (i.e., occurring within secs to 10s of secs of exposure). In contrast, the antibody to the cadherin 23-like polypeptide requires approximately 10 min exposure to significantly decrease vibration sensitivity. At this dilution, the antibody achieves a full inhibition of vibration sensitivity by 15 min exposure. Because the effect of the antibody on reducing vibration sensitivity is gradual, we suspect that the some aspect of the biology of cadherin 23-like polypeptide is dynamic on a relatively slow time scale (i.e., several mins). Three likely protein candidates for interacting with the cadherin-23-like polypeptide would be (1) a self-interaction to form a dimer; (2) an interaction with a different cadherin; or (3) an interaction with the transduction channel. Unpublished data from our laboratory suggest that the third possibility is correct (i.e., that the C-terminus of the cadherin 23-like polypeptide directly interacts with a TRPA1 ion channel). Provided that these preliminary data are confirmed, they will be presented in a separate manuscript.

According to our working model, a pool of 'free' cadherin 23-like polypeptides exists in equilibrium with cadherin 23-like polypeptides incorporated into mechanotransduction apparatus of hair bundles. Cadherin 23-like polypeptides incorporated into the mechanotransduction apparatus eventually exchange places with cadherin 23-like polypeptides in the free pool over a time course of several min. The antibodies may bind to the 'free' cadherin 23-like polypeptides at a site necessary for establishing protein-protein interactions critical to signal transduction. Thus, in the presence of the antibody, the pool of 'free' cadherin 23-like polypeptides normally available to enter functional mechanotransduction apparatus is largely or entirely depleted because of steric hindrance caused by the bound antibody. Consequently, as cadherin 23-like polypeptides exit functional mechanotransduction apparatus to enter the pool, the scarcity of 'free' cadherin 23-like polypeptides available to replace them results in a loss of vibration sensitivity. Ongoing efforts are aimed at testing this model.

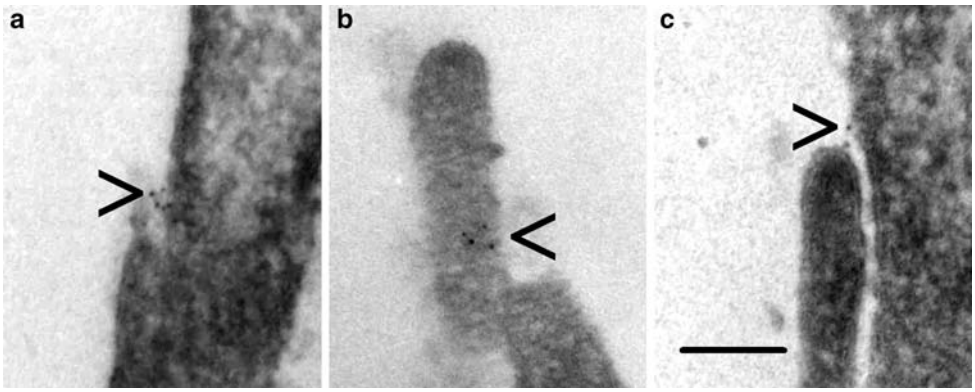

Fig. 9 Cadherin 23-like immunoelectron microscopy of pairs of stereocilia. Tissue from the anemone, *Haliplanella luciae*, was processed for pre-embedment immunoelectron microscopy. Intact pairs of stereocilia having immunogold particles are shown. In **a**, a shorter, small diameter stereocilium lies adjacent to a taller, large diameter stereocilium. A cluster of gold particles is shown on the large diameter stereocilium (*arrowhead*). In **b** a shorter, small diameter stereocilium lies adjacent to a taller, small diameter stereocilium. A cluster of gold particles is shown on the taller stereocilium (*arrowhead*). In **c** a single gold particle is seen at each end of a linkage (*arrowhead*) possibly a tip link, interconnecting a small diameter stereocilium and a taller, large diameter stereocilium. *Scale bar* 0.14 μm

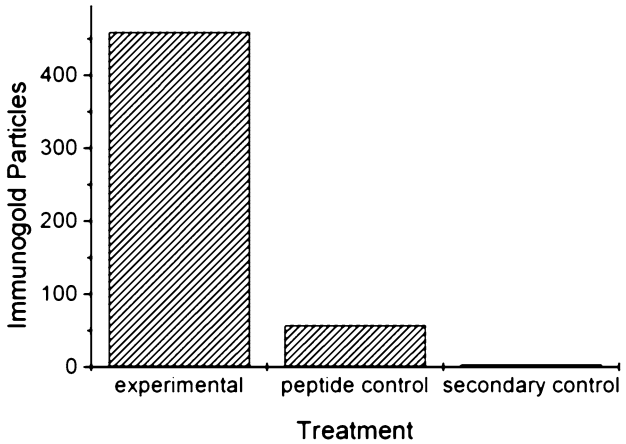

Fig. 10 Specificity of labeling in cadherin 23-like immunoelectron microscopy. Immunogold particles were counted for a comparable area of thin sections of a specimen divided into thirds and processed as follows. The experimental third was processed for routine immunoelectron microscopy; the peptide control was exposed to a combination of the free peptide and antibody; the secondary control was exposed only to the secondary antibody

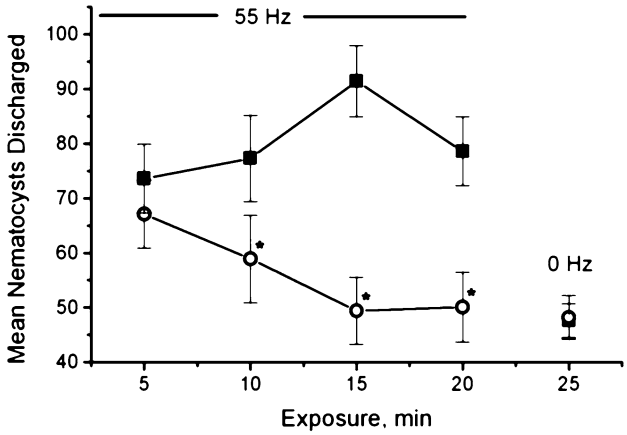

Fig. 11 Effects on nematocyst discharge of the antibody to the cadherin 23-like polypeptide. Tentacles of sea anemones were touched with gelatin-coated, test probes to elicit discharge of nematocysts into them. The test probes were fixed in glutaraldehyde and then examined using phase contrast microscopy. Microbasic p-mastigophore nematocysts were counted for a representative field of view (at ×400 total magnification) for each test probe. Mean numbers of microbasic p-mastigiphore nematocysts counted (±SEM, $n = 10$) is plotted for animals tested at increments following exposure to antibody (*white circles*) or not (untreated controls, *black squares*). For the first 20 min of the experiment, animals were tested in the presence of vibrations at 55 Hz. At 25-min exposure discharge was tested in the absence of vibrations. *Asterisks* indicate significant differences in the data for pair-wise comparisons (i.e., 5 min antibody vs. 5 min control, etc.)

Conclusions

In an evolutionary context, sea anemones are the most primitive animals to possess hair bundle mechanoreceptors. Pharmacological agents that disrupt mechanotransduction in vertebrate hair cells also do so in anemone hair bundles (Watson et al. 1997, 1998a). We here find that a cadherin 23-like polypeptide is present in anemone hair bundles where it may contribute to the structure of tip links. Thus, similarities between anemone hair bundles and hair bundles of vertebrate hair cells may extend to the protein level.

Acknowledgments We appreciate financial support from NSF IOB0542574 and critical comments on the original manuscript by two anonymous reviewers.

References

Abedin M, King N (2008) The premetazoan ancestry of cadherins. Science 319:946–948

Ahmed ZM, Goodyear R, Riazuddin S, Lagziel A, Legan PK, Behra M, Burgess SM, Lilley KS, Wilcox ER, Riazuddin S, Griffith AJ, Frolenkov GJ, Belyantseva IA, Richardson GP, Friedman TB (2006) The tip link antigen, a protein associated with the transduction complex of sensory hair cells, is protocadherin 15. J Neurosci 26:7022–7034

Ashmore JF (1991) The electrophysiology of hair cells. Annu Rev Physiol 53:465–476

Assad JA, Shepherd GM, Corey DP (1991) Tip-link integrity and mechanical transduction in vertebrate hair cells. Neuron 7:985–994

Bolz H, von Brederlow B, Ramirez A, Bryda EC, Kutsche K, Nothwang HG, Seeliger M, Cabrera M, Vila MC, Molina OP (2001) Mutation of CDH23, encoding a new member of the cadherin gene family, causes Usher syndrome type 1D. Nat Genet 27:108–112

Bork JM, Peters LM, Riazuddin S, Bernstein SL, Ahmed ZM, Ness SL, Polomeno R, Ramesh A, Schloss M, Srisailpathy CR (2001) Usher syndrome 1D and nonsyndromic autosomal recessive deafness DFNB12 are caused by allelic mutations of the novel cadherin-like gene CDH23. Am J Hum Genet 68:26–37

Di Palma F, Holme RH, Bryda EC, Belyantseva IA, Pellegrino R, Kachar B, Steel KP, Noben-Trauth K (2001) Mutations in Cdh23, encoding a new type of cadherin, cause stereocilia disorganization in waltzer, the mouse model for Usher syndrome type 1D. Nat Genet 27:103–107

Furness DN, Hackney CM (1985) Cross-links between stereocilia in the guinea pig cochlea. Hear Res 18:177–188

Howard J, Roberts WM, Hudspeth AJ (1988) Mechanoelectrical transduction by hair cells. Annu Rev Biophys Chem 17:99–124

Hudspeth AJ (1985) The cellular basis of hearing: the biophysics of hair cells. Science 230:745–752

Hudspeth AJ (1997) How hearing happens. Neuron 19:947–950

Kachar B, Parrakal M, Kurc M, Zhao Y, Gillespie PG (2000) High-resolution structure of hair-cell tip-links. Proc Natl Acad Sci USA 97:13336–13341

Kazmierczak P, Sakaguchi H, Tokita J, Wilson-Kubalek EM, Milligan RA, Muller U, Kachar B (2007) Cadherin 23 and protocadherin 15 interact to form tip-link filaments in sensory hair cells. Nature 449:87–91

Lagziel A, Ahmed ZM, Schultz JM, Morell RJ, Belyantseva IA, Friedman TB (2005) Spatiotemporal pattern and isoforms of cadherin 23 in wild type and waltzer mice during inner ear hair cell development. Dev Biol 280:295–306

LeMasurier M, Gillespie PG (2005) Hair-cell mechanotransduction and cochlear amplification. Neuron 48:403–415

Mariscal RN (1974) Nematocysts. In: Muscatine L, Lenhoff HM (eds) Coelenterate biology, reviews and new perspectives. Academic, New York, pp 129–178

Michel V, Goodyear RJ, Weil D, Marcotti W, Perfettini I, Wolfrum U, Kros CJ, Richardson GP, Petit C (2005) Cadherin 23 is a component of the transient lateral links in the developing hair-bundles of cochlear sensory cells. Dev Biol 280:281–294

Minasian LL Jr, Mariscal RN (1979) Characteristics and regulation of fission activity in clonal cultures of the cosmopolitan sea anemone, *Haliplanella luciae* (Verrill). Biol Bull 157:478–493

Mire P, Nasse J (2002) Hair bundle motility induced by chemoreceptors in anemones. Hear Res 163:111–120

Mire-Thibodeaux P, Watson GM (1994) Morphodynamic hair bundles arising from sensory cell/supporting cell complexes frequency-tune nematocyst discharge in sea anemones. J Exp Zool 268:281–292

Namimatsu S, Ghazizadeh M, Sugisaki Y (2005) Reversing the effects of formalin fixation with citraconic anhydride and heat: a universal antigen retrieval method. J Histochem Cytochem 53:3–11

Nicolson T, Rusch A, Friedrich RW, Granato M, Ruppersberg JP, Nüsslein-Volhand C (1998) Genetic analysis of vertebrate sensory hair cell mechanosensation: the zebrafish circler mutants. Neuron 20:271–283

Osborne MP, Comis SD, Pickles JO (1988) Further observations on the fine structure of tip links between stereocilia of the guinea pig cochlea. Hear Res 35:99–108

Peteya DJ (1975) The ciliary-cone sensory cell of anemones and cerianthids. Tissue Cell 7:243–252

Pickles JO, Comis SD, Osborne MP (1984) Cross-links between stereocilia in the guinea pig Organ of Corti, and their possible relation to sensory transduction. Hear Res 15:103–112

Preyer S, Hemmert W, Zenner HP, Gummer AW (1995) Abolition of the receptor potential response of isolated mammalian outer hair cells by hair-bundle treatment with elastase: a test of the tip-link hypothesis. Hear Res 89:187–193

Roberts WM, Howard J, Hudspeth AJ (1988) Hair cells: transduction, tuning, and transmission in the inner ear. Annu Rev Cell Biol 4:63–92

Siemens J, Lillo C, Dumont RA, Reynolds A, Williams DS, Gillespie PG, Muller U (2004) Cadherin 23 is a component of the tip link in hair-cell stereocilia. Nature 428:950–955

Slepecky N, Chamberlain SC (1985) The cell coat of inner ear sensory and supporting cells as demonstrated by ruthenium red. Hear Res 17:281–288

Sollner C, Rauch GJ, Siemens J, Geisler R, Schuster SC, Muller U, Nicolson T, Tubingen 2000 Screening Consortium (2004) Mutations in cadherin 23 affect tip links in zebrafish sensory hair cells. Nature 428:955–959

Sotomayor M, Corey DP, Schulten K (2005) In search of the hair cell gating spring: elastic properties of ankyrin and cadherin repeats. Structure 13:669–682

Tsuprun V, Goodyear RJ, Richardson GP (2004) The structure of tip links and kinocilial links in avian sensory hair bundles. Biophys J 87:4106–4112

Watson GM, Hessinger DA (1989) Cnidocyte mechanoreceptors are tuned to the movements of swimming prey by chemoreceptors. Science 243:1589–1591

Watson GM, Mire P (2004) Dynamic tuning of hair bundle mechanoreceptors in a sea anemone during predation. Hydrobiologica 530(531):123–128

Watson GM, Mire P, Hudson RR (1997) Hair bundles of sea anemones as a model system for vertebrate hair bundles. Hear Res 107:53–66

Watson GM, Mire P, Hudson RR (1998a) Repair of hair bundles in sea anemones by secreted proteins. Hear Res 115:119–128

Watson GM, Mire P, Hudson RR (1998b) Frequency specificity of vibration dependent discharge of nematocysts in sea anemones. J Exp Zool 281:582–593

Zhao Y, Yamoah EN, Gillespie PG (1996) Regeneration of broken tip links and restoration of mechanical transduction in hair cells. Proc Natl Acad Sci USA 94:15469–15474